Proceedings of the 17th World Congress
The International Federation of Automatic Control
Seoul, Korea, July 6-11, 2008

Hybrid Adaptive Observer for a Brushless DC Motor

Piotr Niemczyk * **Thomas Porchez** * **Jan Dimon Bendtsen** *
Carsten Skovmose Kallesøe **

* *Department of Electronic Systems, Aalborg University*
Fredrik Bajers Vej 7C, 9220 Aalborg Øst, Denmark
(e-mail: {pn, tpor06, dimon}@es.aau.dk)
** *Grundfos Management A/S*
Poul Due Jensens Vej 7, 8850 Bjerringbro, Denmark
(e-mail: ckallesoe@grundfos.com)

Abstract:
In this paper a novel hybrid adaptive observer for Brushless DC Motors (BLDCM) is presented. It uses two current measurements of BLDCM phases to estimate the angle and the speed of the rotor. The observer is designed on the basis of a hybrid model, which is also presented in this paper. The parameters of the observer are found using an off-line optimization approach. The observer is practically implementable and verified off-line against real measurements.

1. INTRODUCTION

A Brushless DC Motor (BLDCM) is a Permanent Magnet Synchronous Machine (PMSM) with trapezoidal back-EMF. In brushless motors the windings are fixed while the permanent magnet is placed on the rotor. A BLDCM is used when high efficiency and reliability are required, e.g., hard drives, PC cooling fans, electric vehicles. It has a robust and compact design due to the lack of commutator, however, an external controller is required to generate a rotating magnetic field which is followed by the PM. The control generates torque ripples and noise as it is performed by discrete phase switches.

Back-EMF sensing is generally used to estimate the angle of the rotor, which is required to control a BLDCM properly (know when the switches should occur). Although this is a simple and efficient way to estimate the angle, it only gives information at discrete instances. Therefore this paper investigates the possibility of building a dynamical observer to provide better angle resolution, allowing advanced control methods to be used in order to reduce torque ripples.

A BLDCM is driven by an inverter (Fig. 1) which switches the phases depending on the position of the rotor. Such behaviour can be considered as a hybrid system due to the existence of both discrete dynamics (a phase can be activated or deactivated) and continuous dynamics (currents, angle, and angular velocity change smoothly with time). A hybrid model of such a system was presented in Hansen et al. [2007]. However, in this paper a slightly different model structure is used. This is done to improve computation demands of the observer and to enable real time implementation. In the new hybrid model the dynamic equations are described in *ab*-frame, whereas *qd*-frame is generally used to model a three phase PMSM (Krause et al. [1995], Hansen et al. [2007]).

A hybrid adaptive observer is built on basis of the hybrid model. The adaptive approach used in this work is based on Urbański and Zawirski [2004]; compared to that work, the novelty in this paper is that the observer is hybrid and modified to fit presented model description. The parameters for the observer are found using an optimization procedure based on a modified form of evolutionary algorithm (Beyer and Schwefel [2002], Pedersen [2005], Ursem and Vadstrup [2003]).

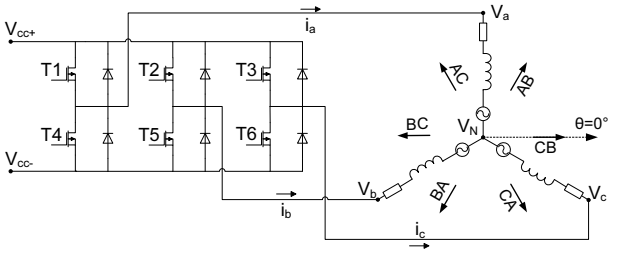

Fig. 1. Electrical schematic of an inverter and a BLDCM, with magnetic fields created by activating each pair of the phases.

The paper presents a step on the way to a fully closed-loop control based on observed feedback for BLDCM. In this work, the observer for a water pump drive is considered. This allows some simplifications while studying the performance.

1.1 BLDCM design

Voltages at the terminals of a BLDCM are generated by switching transistors in the inverter (Fig. 1) according to a commutation scheme. One such scheme, which is commonly used in BLDCM applications is referred to as the 120° voltage source inverter. Fig. 2 shows the control voltages and the corresponding back-EMF of the three phases. The scheme is referred to as a 120° inverter because each phase draws current for approximately 120° of a revolution and is subsequently tristated for 60°, i.e. both transistors of the corresponding inverter leg are closed. The magnitude of the terminal voltage V_{cc} (shown in Fig. 1) is controlled by PWM modulation.

The commutation scheme described above has the drawback that torque ripples are generated if the back-EMF of the BLDCM is not perfectly trapezoidal. Those

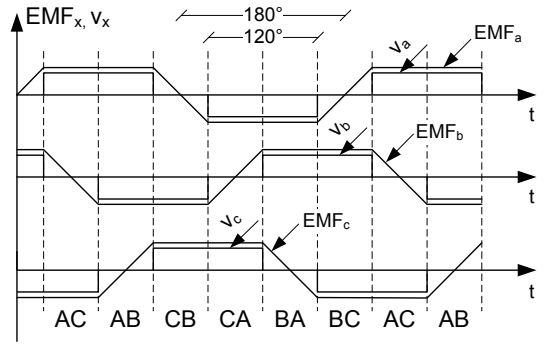

Fig. 2. Idealized voltages applied to the three phases and generated back-EMF over time when using the BLDCM with a 120° inverter.

ripples could be eliminated using more advanced commutation schemes, however, they require reliable and precise information about angle of the rotor. This information could be provided by a tachometer or by the proposed observer.

In the following sections the hybrid model of a BLDCM with an inverter is presented first. Then the hybrid adaptive observer for the rotor angle is derived. Finally, a test scenario is presented in which the observer is running in parallel with a real motor. The paper ends with concluding remarks.

2. HYBRID MODEL OF THE BLDCM

The concept of hybrid modelling of a BLDCM was proposed in Hansen et al. [2007]. The system encounters abrupt changes in dynamical behaviour hence the model consists of continuous equations switched by a Finite State Automaton (FSA). Fig. 3 presents the relations between the continuous and discrete parts of the system.

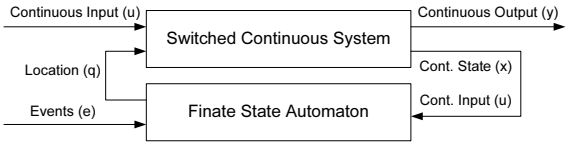

Fig. 3. Relations between the continuous and the discrete part of a hybrid system.

The definition of a hybrid system used in this paper was introduced in Alminde et al. [2006].

Definition 1.
A hybrid system is defined as an 8-tuple:

$$\mathcal{H} = (\mathcal{Q}, X, U, Y, E, \mathcal{F}, \mathcal{G}, \mathcal{T}) \tag{1}$$

where

- $\mathcal{Q} = \{1, 2, \ldots, s\} \subset \mathbb{Z}^+$ is the set of location indexes with cardinal number s,
- $X = \{\mathbf{x} | \mathbf{x} \in X_q : q \in Q, X_q \subseteq \mathbb{R}^{n_q}\}$ is the continuous state-space with dimension $n_{q \in Q} \in \mathbb{Z}^+$,
- $U = \{\mathbf{u} | \mathbf{u} \in U_q : q \in Q, U_q \subseteq \mathbb{R}^{m_q}\}$ is the continuous input-space with dimension $m_{q \in Q} \in \mathbb{Z}^+$,
- $Y = \{\mathbf{y} | \mathbf{y} \in Y_q : q \in Q, Y_q \subseteq \mathbb{R}^{p_q}\}$ is the continuous output-space with dimension $p_{q \in Q} \in \mathbb{Z}^+$,
- $E \subseteq 2^{\Sigma}$ is the set of possible input/output event labels, where Σ is an appropriate set of labels,
- $\mathcal{F} : \mathcal{Q} \times X \times U \to \dot{X}$ is the forcing function on the continuous state-space,
- $\mathcal{G} : \mathcal{Q} \times X \times U \to Y$ is a continuous output map,
- $\mathcal{T} : \mathcal{Q} \times X \times U \times E \to \mathcal{Q} \times X \times E$ is a transition map.

The continuous forcing function $\mathcal{F}$, the output mapping $\mathcal{G}$, and the discrete transition map $\mathcal{T}$ all depend on the discrete location, continuous states and inputs; events e affect only the discrete dynamics.

2.1 Finite State Automaton

A hybrid automaton (HA) for the model is composed knowing the control strategy of the BLDCM and assuming only one direction of rotation, $\omega_e > 0$. This is due to the pump application, which allows simplification of the study ($\omega_e < 0$ follows by symmetry, but note that the model does not allow for standstill, $\omega_e = 0$).

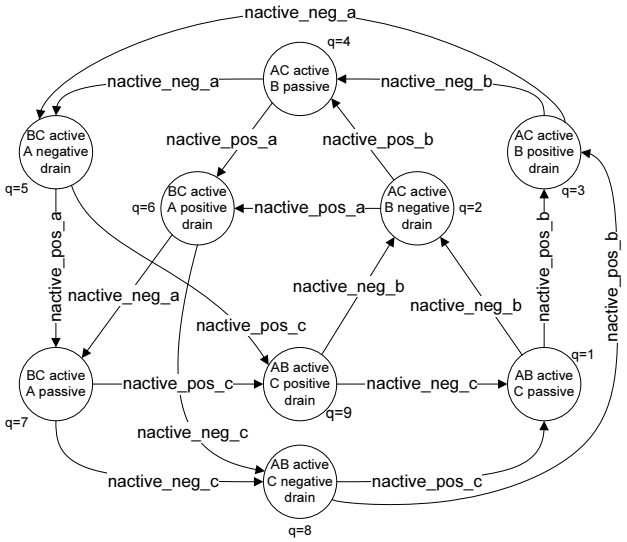

Fig. 4. Finite state automaton of a BLDCM considering $\omega_e > 0$ and given control strategy.

From Fig. 2 it can be seen that when a BLDCM drive is running two stator phases are always active, while the third one is deactivated. After a phase switch, the coil corresponding to the deactivated phase contains energy stored as current. This current has to be drained through the corresponding diodes. In the hybrid automaton (Fig. 4), proper drain states ($q = \{2, 3, 5, 6, 8, 9\}$) are activated before entering another control configuration of phases. This implies that the hybrid automaton consists of three locations where two phases are active $q = \{1, 4, 7\}$, and six locations, where one of the phases is draining. The drain states are distinguished because the input voltage to the tristated phase depends on the sign of the drain current according to (2), where x is the tristated phase.

$$V_x \approx \begin{cases} V_{cc+} & \text{if} \quad i_x < 0 \\ V_{cc-} & \text{if} \quad i_x > 0 \end{cases} \tag{2}$$

The transitions are triggered by events which are generated by the control sequence and detection of zero crossing in the estimate of the draining current. For instance, event nactive_neg_a means that the phase a is deactivated and the draining current is negative, and nactive_pos_a means phase a deactivated and positive current. In the model, the draining stage is finished when a

zero-crossing is detected in the current estimate (changes from nactive_neg_a to nactive_pos_a and vice versa).

In an extreme situation, it may occur that there is not enough time for draining the current in deactivated coil, and the hybrid automaton switches only between drain phases. This is also included in the automaton by adding transitions between the states $q = \{2, 3, 5, 6, 8, 9\}$.

2.2 Continuous Equations

The electrical dynamics of the BLDCM are derived on basis of Fig. 1, which shows that a phase can be considered as a serial connection of an inductance, a resistance, and a back-EMF (Krause et al. [1995]):

$$\mathbf{V}_{abc} - \mathbf{V}_N = \underbrace{\mathbf{L}\frac{d}{dt}\mathbf{i}_{abc}}_{Inductance} + \underbrace{r\,\mathbf{i}_{abc}}_{Resistance} + \underbrace{(\frac{d}{d\theta_e}\boldsymbol{\lambda'}_m)\omega_e}_{Back-EMF} \quad (3)$$

where $\mathbf{V}_{abc} = [V_a\ V_b\ V_c]^T$ is the vector of input voltages, $\mathbf{V_N}$ is a vector containing the neutral node voltage as the elements, and $\mathbf{i}_{abc} = [i_a\ i_b\ i_c]^T$ is the vector of currents through the phases. r is the resistance of a phase and the inductance matrix $\mathbf{L}$ is defined as follows (L_l is the leakage inductance, and L_m is the magnetizing inductance):

$$\mathbf{L} = \begin{bmatrix} L_l + L_m & -\frac{1}{2}L_m & -\frac{1}{2}L_m \\ -\frac{1}{2}L_m & L_l + L_m & -\frac{1}{2}L_m \\ -\frac{1}{2}L_m & -\frac{1}{2}L_m & L_l + L_m \end{bmatrix} \quad (4)$$

$\boldsymbol{\lambda'}_m$ is the vector of the stator flux linkages created by the PM and is a periodic function of the rotor position. The BLDCM being designed to have a symmetric trapezoidal back-EMF, $\boldsymbol{\lambda'}_m$ can be decomposed in a series of odd harmonics. It is assumed that the third order decomposition is sufficient. With λ'^1_m the magnitude of the first harmonic and N_3 the magnitude of the third harmonic relative to the fundamental, the derivative of the vector of flux linkages is expressed as follows

$$\frac{d}{d\theta_e}\boldsymbol{\lambda'}_m = \lambda'^1_m \begin{bmatrix} \cos(\theta_e) + 3N_3\cos(3\theta_e) \\ \cos(\theta_e - \frac{2\pi}{3}) + 3N_3\cos(3\theta_e) \\ \cos(\theta_e + \frac{2\pi}{3}) + 3N_3\cos(3\theta_e) \end{bmatrix} \quad (5)$$

In the drain stage all three phases are active. Applying Kirchoff's current law defines a constraint on the currents: $i_c = -i_a - i_b$. Incorporating this constraint in (3) and eliminating the neutral node voltage $\mathbf{V_N}$, the following model is obtained:

$$\frac{d}{dt}\mathbf{i}_{ab} = -\frac{r}{L}\mathbf{i}_{ab} - \frac{\lambda'^1_m}{L}\begin{bmatrix} 1 & 0 \\ -\frac{1}{2} & \frac{\sqrt{3}}{2} \end{bmatrix}\begin{bmatrix} e_\alpha \\ e_\beta \end{bmatrix} + \frac{1}{L}\begin{bmatrix} \frac{2}{3} & -\frac{1}{3} & -\frac{1}{3} \\ -\frac{1}{3} & \frac{2}{3} & -\frac{1}{3} \end{bmatrix}\mathbf{V}_{abc}\,, \quad (6)$$

where $\mathbf{i}_{ab} = [i_a\ i_b]^T$, $L = L_l + \frac{3}{2}L_m$ is the equivalent inductance of a phase, and $e_\alpha = \omega_e\cos\theta_e$, $e_\beta = \omega_e\sin\theta_e$ correspond to the back-EMF. This equation describes the electrical dynamics in all drain stages of the BLDCM. The only differences between these stages are the supply voltages, generated by the control, and the sign of the drain current. The voltage in the deactivated phase is given by (2).

In case there is no current in the draining phase (two phases active), the description changes. When phase a and b is active, $i_c = 0$ and the constraint becomes $i_a = -i_b$. The following model is obtained:

$$\frac{d}{dt}i_a = -\frac{r}{L_s}i_a - \frac{\lambda'^1_m}{L_s}\begin{bmatrix} \frac{3}{4} & -\frac{\sqrt{3}}{4} \end{bmatrix}\begin{bmatrix} e_\alpha \\ e_\beta \end{bmatrix} + \frac{1}{L_s}\begin{bmatrix} \frac{1}{2} & -\frac{1}{2} & 0 \end{bmatrix}\mathbf{V}_{abc} \quad (7)$$

Similar equations can be determined for the remaining locations of the hybrid automaton.

2.3 Formal description

Hybrid system according to Definition 1 is expressed as follows:

- There are 9 discrete locations.
$$\mathcal{Q} = \{1, 2, 3, 4, 5, 6, 7, 8, 9\}$$
- The state vector x and the input vector u are the same in all the locations, in order to keep a uniform representation. The state vector consists of two stator currents i_a and i_b, and the two values corresponding to the back-EMF e_α and e_β. The input vector u consists of three phase input voltages V_a, V_b and V_c.
$$X_q = \left\{\mathbf{x} = [\,i_a\ i_b\ e_\alpha\ e_\beta\,]^T\right\} \subset \mathbb{R}^4, \forall q \in \mathcal{Q}$$
$$U_q = \left\{\mathbf{u} = \mathbf{V}_{abc} = [\,V_a\ V_b\ V_c\,]^T\right\} \subset \mathbb{R}^3, \forall q \in \mathcal{Q}$$
- The continuous outputs of the system are the two measured currents i_a and i_b.
$$Y_q = \left\{\mathbf{y} = \mathbf{i}_{ab} = [\,i_a\ i_b\,]^T\right\} \subset \mathbb{R}^2, \forall q \in \mathcal{Q}$$
- There are six events that trigger the transitions.
$$E = \{\text{nactive\_neg\_x},\ \text{nactive\_pos\_x} \mid \text{x} \in \{\text{a, b, c}\}\}$$
- The forcing function on the continuous state-space is presented in (8), with $\mathcal{J} = \begin{bmatrix} 0 & -1 \\ 1 & 0 \end{bmatrix}$. $\mathcal{F}$ is found by applying (6) with the particular properties of each location of the automaton and knowing that:
$$\dot{e}_\alpha = \frac{d}{dt}\omega_e\cos\theta_e = \frac{\dot{\omega}_e}{\omega_e}e_\alpha - \omega_e e_\beta$$
$$\dot{e}_\beta = \frac{d}{dt}\omega_e\sin\theta_e = \frac{\dot{\omega}_e}{\omega_e}e_\beta + \omega_e e_\alpha$$
- The continuous output map is not dependent on the discrete state as the continuous state and output remain the same.
$$\mathcal{G} : \mathbf{y} = \begin{bmatrix}\mathbf{I}^{2\times 2}\ \mathbf{0}\end{bmatrix}\mathbf{x}, \forall q \in \mathcal{Q}$$
- The transition map $\mathcal{T}$ is defined using the value of the current discrete state and an event to determine what is the next discrete state. There are no reset functions and no events generated during a transition. Therefore $\mathcal{T}$ is defined as $\mathcal{T} : \mathcal{Q} \times E \to \mathcal{Q}$. To define $\mathcal{T}$ the following notation is used: $(q_{\text{current}}, e_{\text{received}}) \to q_{\text{new}}$, where q_{current} is the current value of the discrete state, e_{received} is the event that triggers the transition, and q_{new} is the new value of the discrete state.

$$\mathcal{F}: \begin{cases} \dot{\mathbf{x}}_q = \begin{bmatrix} -\frac{r}{L}\mathbf{I}^{2\times 2} & -\frac{\lambda'^1_m}{L}\begin{bmatrix} 1 & 0 \\ \frac{1}{2} & \frac{\sqrt{3}}{2} \end{bmatrix} \\ \mathbf{0} & \mathcal{J}\omega_e + \frac{\dot{\omega}_e}{\omega_e}\mathbf{I}^{2\times 2} \end{bmatrix} \mathbf{x}_q + \frac{1}{L}\begin{bmatrix} \frac{2}{3} & -\frac{1}{3} & -\frac{1}{3} \\ -\frac{1}{3} & \frac{2}{3} & -\frac{1}{3} \\ \multicolumn{3}{c}{\mathbf{0}} \end{bmatrix} \mathbf{u}_q & \text{if } q \in \{2,3,5,6,8,9\} \\ \dot{\mathbf{x}}_q = \begin{bmatrix} -\frac{r}{L}\mathbf{I}^{2\times 2} & -\frac{\lambda'^1_m}{L}\begin{bmatrix} \frac{3}{4} & -\frac{\sqrt{3}}{4} \\ -\frac{3}{4} & \frac{\sqrt{3}}{4} \end{bmatrix} \\ \mathbf{0} & \mathcal{J}\omega_e + \frac{\dot{\omega}_e}{\omega_e}\mathbf{I}^{2\times 2} \end{bmatrix} \mathbf{x}_q + \frac{1}{L}\begin{bmatrix} \frac{1}{2} & -\frac{1}{2} & 0 \\ -\frac{1}{2} & \frac{1}{2} & 0 \\ \multicolumn{3}{c}{\mathbf{0}} \end{bmatrix} \mathbf{u}_q & \text{if } q = 1 \\ \dot{\mathbf{x}}_q = \begin{bmatrix} -\frac{r}{L}\mathbf{I}^{2\times 2} & -\frac{\lambda'^1_m}{L}\begin{bmatrix} \frac{3}{4} & -\frac{\sqrt{3}}{4} \\ 0 & 0 \end{bmatrix} \\ \mathbf{0} & \mathcal{J}\omega_e + \frac{\dot{\omega}_e}{\omega_e}\mathbf{I}^{2\times 2} \end{bmatrix} \mathbf{x}_q + \frac{1}{L}\begin{bmatrix} \frac{1}{2} & 0 & -\frac{1}{2} \\ \multicolumn{3}{c}{\mathbf{0}} \end{bmatrix} \mathbf{u}_q & \text{if } q = 4 \\ \dot{\mathbf{x}}_q = \begin{bmatrix} -\frac{r}{L}\mathbf{I}^{2\times 2} & -\frac{\lambda'^1_m}{L}\begin{bmatrix} 0 & 0 \\ 0 & \frac{\sqrt{3}}{2} \end{bmatrix} \\ \mathbf{0} & \mathcal{J}\omega_e + \frac{\dot{\omega}_e}{\omega_e}\mathbf{I}^{2\times 2} \end{bmatrix} \mathbf{x}_q + \frac{1}{L}\begin{bmatrix} 0 & 0 & 0 \\ 0 & \frac{1}{2} & -\frac{1}{2} \\ \multicolumn{3}{c}{\mathbf{0}} \end{bmatrix} \mathbf{u}_q & \text{if } q = 7 \end{cases} \tag{8}$$

$$\mathcal{T}: \begin{cases} (1, \text{nactive\_neg\_b}) \to 2 \;\; (1, \text{nactive\_pos\_b}) \to 3 \\ (2, \text{nactive\_pos\_b}) \to 4 \;\; (2, \text{nactive\_pos\_a}) \to 6 \\ (3, \text{nactive\_neg\_b}) \to 4 \;\; (3, \text{nactive\_neg\_a}) \to 5 \\ (4, \text{nactive\_neg\_a}) \to 5 \;\; (4, \text{nactive\_pos\_a}) \to 6 \\ (5, \text{nactive\_pos\_a}) \to 7 \;\; (5, \text{nactive\_pos\_c}) \to 9 \\ (6, \text{nactive\_neg\_a}) \to 7 \;\; (6, \text{nactive\_neg\_c}) \to 8 \\ (7, \text{nactive\_pos\_c}) \to 9 \;\; (7, \text{nactive\_neg\_c}) \to 8 \\ (8, \text{nactive\_pos\_c}) \to 1 \;\; (8, \text{nactive\_pos\_b}) \to 3 \\ (9, \text{nactive\_neg\_c}) \to 1 \;\; (9, \text{nactive\_neg\_b}) \to 2 \end{cases}$$

3. HYBRID OBSERVER

The derived observer is hybrid and adaptive. The idea of an adaptive observer for a BLDCM was introduced in Urbański and Zawirski [2004]. In this paper its structure is changed to fit the model description presented above, which has a hybrid form. The location automaton for the observer is the same as the hybrid automaton for the hybrid model. This is because it is assumed that a startup procedure has already been executed, aligning the rotor to a known position, thus the initial state is known. The electrical angular velocity ω_e is considered a time-varying parameter, therefore equations representing the mechanical dynamics of BLDCM are not used. The observer is proposed for a water pump application drive, where the rotational speed is not varying very rapidly and thus it is assumed that $\dot{\omega}_e = 0$. Furthermore, pumps usually operate at more than half of the full speed (in this case $\omega_r \in [500; 1000]$ [rpm]), which allows to neglect the influence of stiction.

3.1 Structure

The structure of the observer is shown in Fig. 5, where the estimates of θ_e and ω_e are computed using the states $e_\alpha = \omega_e \cos\theta_e$ and $e_\beta = \omega_e \sin\theta_e$:

$$\omega_e = \sqrt{e_\alpha^2 + e_\beta^2}$$

$$\theta_e = \begin{cases} \arccos\left(\frac{e_\alpha}{\omega_e}\right) & \text{for } \frac{e_\beta}{\omega_e} \geq 0 \\ 2\pi - \arccos\left(\frac{e_\alpha}{\omega_e}\right) & \text{for } \frac{e_\beta}{\omega_e} < 0 \end{cases}$$

The estimation of ω_e is fed back to the state estimation as it is the time-varying parameter.

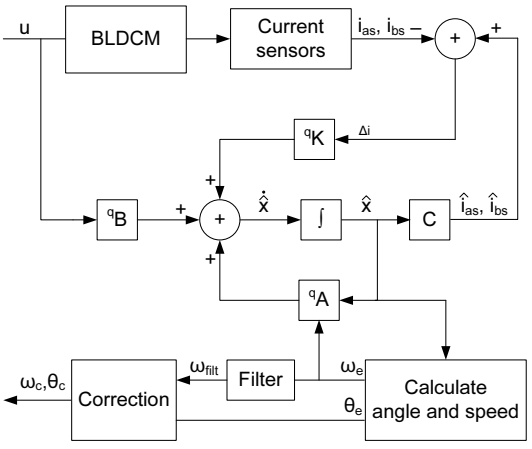

Fig. 5. Structure of the hybrid adaptive observer.

3.2 Continuous time equations of the observer

From the values of the measurements (i_a and i_b) and the estimated states ($\hat{i}_a$ and $\hat{i}_b$), an error vector is defined:

$$\tilde{\mathbf{i}} = \begin{bmatrix} \hat{i}_a - i_a \\ \hat{i}_b - i_b \end{bmatrix}$$

The designed observer has a only proportional feedback correction and is defined as follows:

$$\dot{\hat{\mathbf{x}}} = \underbrace{\mathcal{F}(q, \hat{\mathbf{x}}, \mathbf{V}_{abc})}_{\text{Prediction (Model)}} + \underbrace{{}^{q}\mathbf{K} \cdot \tilde{\mathbf{i}}}_{\text{Correction}} = {}^{q}\mathbf{A}\hat{\mathbf{x}} + {}^{q}\mathbf{B}\hat{\mathbf{u}} + {}^{q}\mathbf{K}\tilde{\mathbf{i}}$$

where ${}^{q}\mathbf{K}$ is the proportional feedback matrix for the location q and ${}^{q}\mathbf{A}$, ${}^{q}\mathbf{B}$ are given in (8). The elements of ${}^{q}\mathbf{K}$ map the error in a current estimation i_x to the derivative of a state $\hat{x}_j$. They are set to zero if the current i_x has no influence on the state. The set of observer coefficients (k_1 to k_{14}) in the following form has to be determined:

$$\text{for } q \in \{2,3,5,6,8,9\} \quad {}^{q}\mathbf{K} = \begin{bmatrix} k_1 & 0 \\ 0 & k_2 \\ k_3 & k_4 \\ 0 & k_5 \end{bmatrix} \qquad \text{for } q = 1 \quad {}^{q}\mathbf{K} = \begin{bmatrix} k_6 & 0 \\ 0 & k_7 \\ k_8 & 0 \\ k_9 & 0 \end{bmatrix}$$

$$\text{for } q = 4 \quad {}^{q}\mathbf{K} = \begin{bmatrix} k_{10} & 0 \\ 0 & 0 \\ k_{11} & 0 \\ k_{12} & 0 \end{bmatrix} \qquad \text{for } q = 7 \quad {}^{q}\mathbf{K} = \begin{bmatrix} 0 & 0 \\ 0 & k_{13} \\ 0 & 0 \\ 0 & k_{14} \end{bmatrix}$$

This is a non-trivial problem and therefore it is useful to employ optimization techniques to determine ${}^{q}\mathbf{K}$.

3.3 Optimization

Determination of observer's feedback parameters using optimization method was used in Urbański and Zawirski [2004]. It is desired to find the coefficients that minimize a cost function Q, which represents the performance of the observer. The function is defined as follows:

$$Q = \underbrace{\left| \int_t^{t+\tau} e_\theta(t)dt \right|}_{Mean} + \underbrace{\int_t^{t+\tau} e_\theta^2(t)dt}_{Variance}$$

where e_θ is the error of estimation in the angle θ_e and $[t; t+\tau]$ is the time range for which the cost function is calculated (should include transient and steady state part of a response, and not include zero for which the system is not observable). This cost function is chosen as it represents the sum of the mean value of the error and its variance.

Value of Q is calculated for a set of parameters k. The observer estimates the electrical angle θ_e for the time period $[t; t+\tau]$ and compares it with actual plant response. The data used for the optimization correspond to a speed step to 500 [rpm]. The feedback coefficients are therefore optimized for this speed. Since there is noise in the measured signals used for the optimization, the value of cost function Q will not converge to zero. The optimization should be finished when the observer reflects the dynamical behaviour of the system. Zero cost function would mean that the observer is optimized for the noise which is not desired.

Random Weight Change (RWC) (Urbański and Zawirski [2004]), Nonlinear Simplex Search (NSS) (Wang and Qiu), and three different Evolutionary Algorithms (EA) (Beyer and Schwefel [2002], Pedersen [2005], and Ursem and Vadstrup [2003]) have been applied to the problem of finding the k parameters. The result of this study is that a good strategy for finding the feedback parameters of the observer is to use RWC to find a region of a minimum, and from there use the Differential Evolution (DE) algorithm (Ursem and Vadstrup [2003]) to find the local minimum. It may sometimes be necessary to run the algorithm a few times as it could converge to a local minimum that is not good enough for the observer.

Table 1 lists the feedback parameters found after optimization.

k_1 to k_5	-1217	-8.79	1101	-5187	8236
k_6 to k_{10}	-18.34	18.93	20627	-64480	-583.7
k_{11} to k_{14}	89890	2060	-74.8	24389	-

Table 1. Table of feedback coefficients.

3.4 Improvement of the estimates

Having the feedback coefficients found by the optimization, the precision of the estimation can be improved. First, the estimate ω_e is filtered by a first order low-pass filter with a cut-off frequency $\omega_{cut} = 20$ [rad/s] (Fig. 7).

From Fig. 6 and 7 is seen that the mean values of the estimation errors are strongly correlated with the value of the angular velocity. At $\omega_{filt} = 160\,[\text{rad} \cdot \text{s}^{-1}]$, the mean value of the error is zero as the optimization was realized for this speed. When the speed increases, the mean value of the error also increases (proportionally). To compensate for this, an offset correction is introduced, yielding new estimates ω_c and θ_c:

$$\omega_c = \omega_{filt} - \alpha(\omega_{filt} - 160)$$
$$\theta_c = \theta_e - \beta(\omega_{filt} - 160)$$

The parameters $\alpha = 0.24$ and $\beta = 0.0015$ are determined from the estimation error as a function of angular velocity.

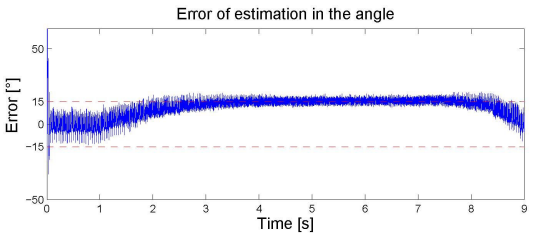

Fig. 6. Error of θ_e angle estimation (before the correction).

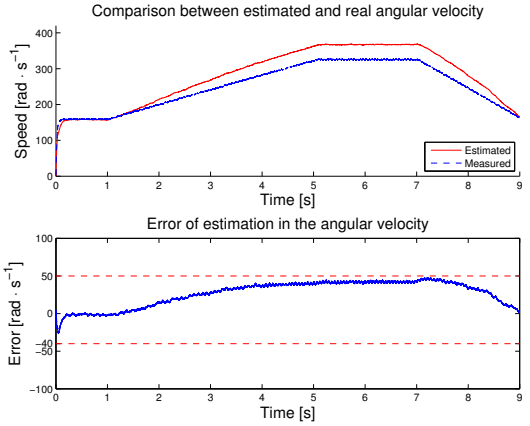

Fig. 7. Error of speed estimation ω_{filt} (after low-pass filtering, but before the correction).

4. TEST RESULTS

The observer was tested using a BLDCM with the following parameters: $r = 3.8\,[\Omega]$, $L = 13.5\,[\text{mH}]$, $\lambda_m^{\prime 1} = 0.2225\,[\frac{\text{V}\cdot\text{s}}{\text{rad}}]$, $J = 0.002\,[\text{kg}\cdot\text{m}^2]$ and $B_m = 5 \times 10^{-4}\,[\text{kg}\cdot\text{m}^2\cdot\text{s}^{-1}]$ and with motor load on the motor. Measurements were acquired using the dSpace® platform while operating the motor in closed loop. The inputs and the two stator currents i_a and i_b were recorded and fed off-line to the observer to examine the tracking performance of the estimation. The measured speed of the motor during the test scenario can be seen in Fig. 9. It includes step input, increase and decrease of the velocity and steady state performance at the maximum and minimum considered velocities.

The results of the verification are depicted in Fig. 8 and 9. The mean value of the estimation error converges quickly to zero and the observer is able to track changes in the whole speed region. The precision of angle estimation remains $\pm 10\,[°]$, while speed estimation precision is $\pm 12\,[\text{rad}\cdot\text{s}^{-1}]$. It is noticed that the precision decreases when the speed varies. This is due to the fact, that the derivative of the speed was assumed to be zero in the equations. When the speed is steady the estimates become more accurate. It can be noticed that the precision at 1000 [rpm] is particularly good and is in range of $\pm 3\,[°]$ electrical degrees.

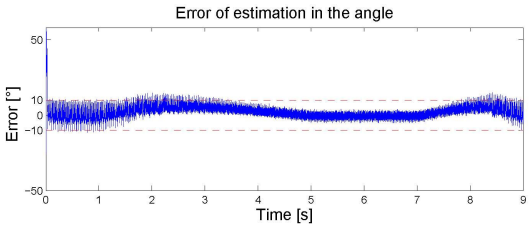

Fig. 8. Error of θ_c angle estimation.

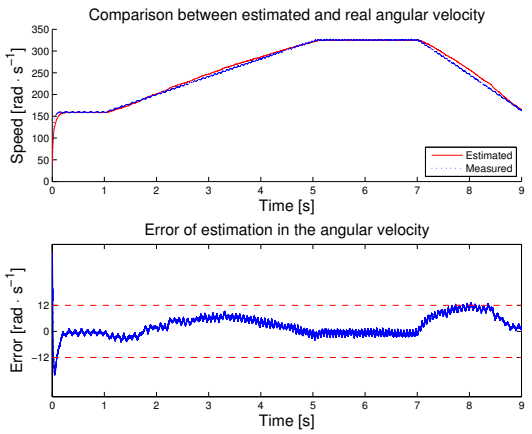

Fig. 9. Comparison between real and estimated (ω_c) speed. Note the different error axis scale.

5. CONCLUSION

In this paper a new hybrid model for a BLDCM was derived. This model is based on continuous time equations and does not require a *qd* transformation. The continuous time equations were subsequently embedded in a hybrid automaton to accommodate the discrete behaviour of the actual system. Tests of the model showed good performance, close to that of a real motor.

Furthermore, it was shown that the model can be used for design of an accurate hybrid observer for estimating the rotation angle and speed of a BLDCM. This means that the position sensor can be omitted using the proposed observer and only the use of two current sensors is required. The observer also provides an estimate of the angular velocity with a precision of $\pm 12\,[\text{rad/s}]$, which can be used as a feedback in a speed controller.

Future work should concentrate on a real time implementation and closed loop application of the observer. It should be verified if it is possible to replace motor's tachometer by the observer. The effects of load changes on the motor should also be investigated.

REFERENCES

Lars Alminde, Karl Kaas Laursen, and Jan Dimon Bendtsen. *A Reusable Software Architecture for Small Satellite AOCS Systems*. Small Satellite Systems and Services Conference, Greece, 2006.

Hans-Georg Beyer and Hans-Paul Schwefel. Evolution strategies - A comprehensive introduction. *Natural Computing*, 1(1), 2002. ISSN 1572-9796.

Hans Brink Hansen, Carsten Skovmose Kallesøe, and Jan Dimon Bendtsen. A hybrid model of a Brushless DC Motor. *IEEE International Conference on Control Applications*, 2007.

Paul C. Krause, Oleg Wasynczuk, and Scott D. Sudhoff. *Analysis of Electric Machinery*. IEEE PRESS, 1995. ISBN 0-7803-1101-9.

Gerulf K. M. Pedersen. *Towards Automatic Controller Design using Multi-Objective Evolutionary Algorithms*. PhD thesis, Department of Control Engineering - Aalborg University, 2005.

Konrad Urbański and Krzysztof Zawirski. Adaptive observer of rotor speed and position for PMSM sensorless control system. *COMPEL: The International Journal for Computation and Mathematics in Electrical and Electronic Engineering*, 23, 2004.

Rasmus K. Ursem and Pierré Vadstrup. Parameter identification of induction motors using differential evolution. *Proceedings of the Fifth Congress on Evolutionary Computation*, pages 790–796, 2003.

Fang Wang and Yuhui Qiu. Multimodal function optimizing by a new hybrid nonlinear simplex search and particle swarm algorithm. *Lecture notes in computer science*. ISSN 0302-9743.